

Graphene: Characterization After Mechanical Exfoliation

Charlotte Reeves

Research Advisor: R. A. Lukaszew

April, 2010

Abstract

The purpose of this experiment was to produce and characterize samples of graphene, defined as a one-atom layer of hexagonally bonded carbon atoms, using a method of mechanical exfoliation. This was done by following the work of K. S. Novoselov in the group of A. K. Geim at the University of Manchester (2004) using Scotch tape to pull apart the layers of a piece of highly oriented pyrolytic graphite (HOPG) and transfer layers from the graphite onto a SiO₂ substrate. These samples were then inspected using an optical microscope in an attempt to discover any thin flakes that might contain sections of single-layer graphene. Nine thin flakes with lengths up to 17 μm were determined to be likely candidates, and two of these plus three others were analyzed using Raman spectroscopy at NASA Langley using a laser of wavelength 532 nm. From these it was determined that a graphene flake two atomic layers thick had been produced.

1. Introduction and Theory Overview

a. An overview of graphene

Nature has produced 3-D materials such as graphite which are composed of many stacked layers of 2-D planar materials. In general, 2-D materials are rarely found in nature because of their instability; thin films, for instance, can become thermodynamically unstable and decompose or segregate below a certain thickness, and in other materials single layers appear only as transient states [1]. Graphene, however, is a notable exception. Graphene is defined as a single one-atom layer of hexagonally bonded carbon atoms (see Figure 1), while graphite is composed of many stacked graphene layers [2].

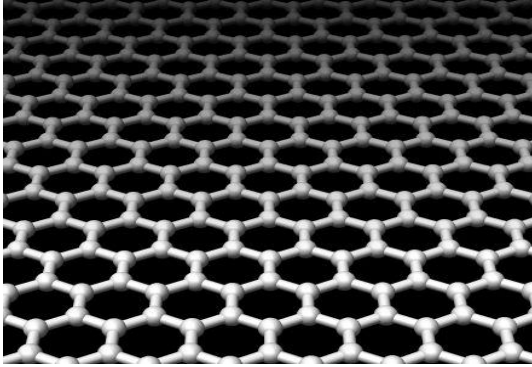


Figure 1: Schematics of graphene structure.

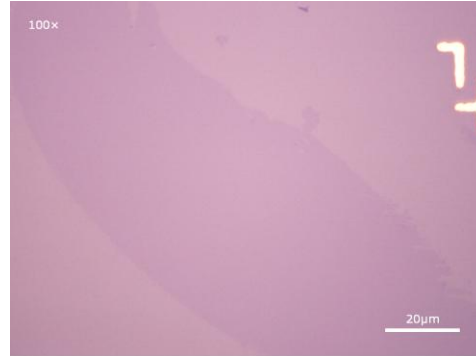


Figure 2: Graphene sample from grapheneindustries.com

The bonding forces between these planes are much weaker than the bonding between the carbon atoms within the planes. The carbon atoms within each sheet of graphene are bonded together via strong covalent bonds, while in graphite those sheets are held together by van der Waals (dipole-dipole) forces, which are much, much weaker. Because graphite is more weakly bound between the layers of carbon atoms, these layers can easily be removed from a bulk sample. In this experiment we use highly oriented pyrolytic graphite (HOPG), which is defined as “artificially grown graphite with an almost perfect alignment perpendicular to the carbon planes” – a synthetic carbon crystal [3].

Graphene possesses some very interesting unique properties; it has a particularly high electron mobility [4], a breaking strength 200 times that of steel [5], a high thermal conductivity [6], and an opacity high enough that it can be seen on a suitable substrate with a standard optical microscope [7] (see Figure 2). These properties, among others, have shown it to have great potential in a number of interesting fields, including in electronics in the construction of graphene transistors [8], integrated circuits, and ultracapacitors (due to their high conductivity) [9].

The most explored aspect of graphene physics is its electronic properties. Charge carriers in condensed matter physics are normally described by the Schrödinger equation with an effective mass m^* different from the free-electron mass. Relativistic particles in the limit of zero rest mass follow the Dirac equation, charge carriers in graphene are called massless Dirac fermions. Electrons propagating through the honeycomb lattice completely lose their effective mass, which results in quasi-particles that are described by a Dirac-like equation rather than the Schrödinger equation. Electron waves in graphene propagate within a layer that is only one atom

thick, which makes them accessible and amenable to various scanning probes as well as sensitive to the proximity of other materials such as high-k dielectrics, superconductors, ferromagnets, etc. Graphene exhibits an astonishing electronic quality. Its electrons can cover submicrometer distances without scattering, even in samples placed on an atomically rough substrate, covered with adsorbates, and at room temperature. As a result of the massless carriers and little scattering, quantum effects in graphene are robust and can survive even at room temperature. The transport properties of real graphene devices have turned out to be much more complicated than theoretical quantum electrodynamics predicts, and some basic questions about graphene's electronic properties have yet to be answered. For example, there is no consensus about the scattering mechanism that currently limits the mobility, and in addition, this property seems to strongly depend on the type of graphene sample been investigated (i.e. exfoliated or prepared via thermal desorption of Si in SiC).

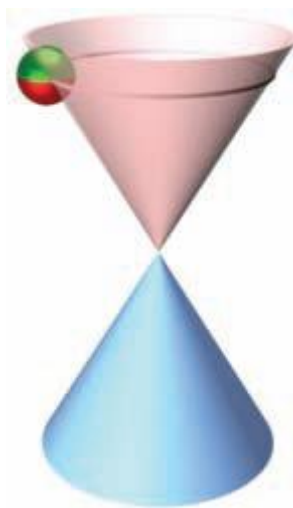


Figure 3: Conical band meeting at a Dirac point

However, graphene itself was only first described relatively recently, initially appearing in the literature in Mouras, S. (1987). So, while other production methods are being used such as epitaxial growth, chemical vapor deposition, and chemical exfoliation [2], mechanical exfoliation, which was introduced in 2004, is still the method which consistently produces high-quality samples with the best properties, though of a limited size. Members in the Lukaszew research group are exploring epitaxial growth on silicon carbide as a different method of graphene production. My objective for the first semester was to create a number of graphene samples from HOPG so that the quality of the graphene I make using the more common method

of mechanical exfoliation can be compared to the graphene they produce using an alternative method

b. An overview of Raman spectroscopy

Raman spectroscopy is one method currently used to determine how many layers of graphene are present in a present sample. It utilizes the process of Raman scattering to identify what materials are present in a specific sample by analyzing the shift in wavelength of light that is scattered off of a material, which is different for different materials.

There are two primary types of scattering that occur when light strikes a material: Rayleigh and Raman scattering. In Rayleigh scattering, a photon of a given energy and wavelength interacts with a molecule in a material and raises it to a virtual energy state. After a moment, the molecule comes back down to its original energy state, releasing another photon. Since the molecule came back down to its original energy state after being raised, the released photon has the same energy (and thus wavelength) as the incident photon; thus, Rayleigh scattering can be referred to as an elastic process (the energy of the photon being conserved).

In Raman scattering, a photon of a given energy and wavelength also interacts with a molecule in a material and raises it to a virtual energy state, as in Rayleigh scattering. However, when the molecule drops from its virtual energy state, it may drop not to its original state but to a state above or below its original energy state. When the molecule drops to a lower state it releases a photon; however, the energy of the photon is *not* the same as that of the incident photon. The energy of the released photon is dependent on the final energy state of the molecule. If the final energy state of the molecule is greater than its original ground state, then the released photon will have a lower energy than the incident photon, and thus a longer wavelength; this is referred to as Stoke's Raman scattering. However, if the final energy state of the molecule is lower than the original initial state, then the released photon will have a higher energy than the incident photon, and thus a shorter wavelength – anti-Stokes Raman scattering. Since the energy of the photons is not conserved, Raman scattering is a form of inelastic scattering. See Figure 4 for a visual representation of all three types of scattering and the differences between their elastic and inelastic properties.

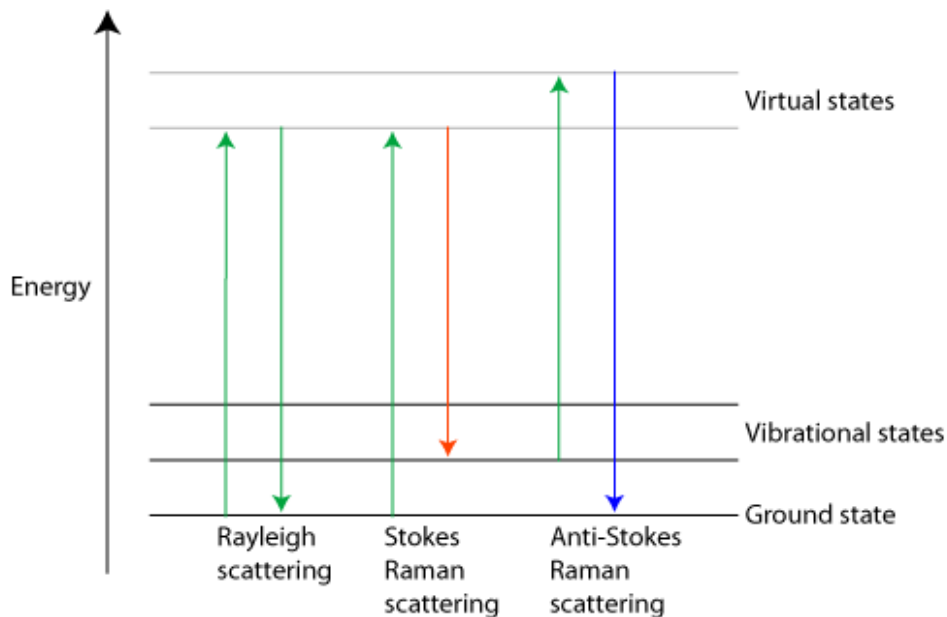


Figure 4: The three forms of scattering
http://www.doitpoms.ac.uk/tlplib/raman/raman_scattering.php

In both types of Raman scattering, the energy removed from or transferred to the photon is related to specific phonons – i.e. lattice vibrations- of the target material. Thus, only certain changes in photon energy, and thus wavelength and frequency, are possible. These frequency shifts are different for every material, which means that measurements of the shift in frequencies in the scattered photons can shed light on the identity of the material in question. The shift depends on the energy of the spacing of the molecule’s modes. However, not all modes appear in the Raman spectra, only those that do involve changes in the polarizability, α , of the molecule being analyzed. The polarizability depends upon the bond lengths in the molecule, with shorter bonds being more difficult to polarize. In crystalline solids, the modes are determined by the crystal structure, which can be determined from the polarization of the scattered light. If the polarizability of a molecule is changing, then the molecule is vibrating, which induces a dipole moment. Oscillating dipole moments release photons, and that in conjunction with changing polarizabilities produces Stokes and anti-Stokes scattering.

Rayleigh scattering occurs much more frequently than either Stokes or anti-Stokes Raman scattering, and Stokes marginally more often than anti-Stokes. With Stokes and anti-Stokes shifts, the shift in photon energy will be the same either way. Thus, Stokes scattering is

usually used in Raman spectroscopy measurements due to its marginally higher frequency of occurrence compared to anti-Stokes scattering.

Raman spectroscopy has significant advantages over other types of spectroscopy (such as infrared) for many reasons: it's non-destructive, does not require any sample preparation, does not require a vacuum, can produce results quickly, "can produce spatially resolved maps of the different forms of carbon within a specimen" [10], and can be used on solids, liquids, gases, and aqueous solutions (infrared spectroscopy readings are complicated by readings of the water solute). It can also be used in a wide range of temperatures and pressures [11] and on small sample areas [10]. Fiber optic cables can also be used to transmit readings, which is useful for remote testing. However, Raman spectroscopy cannot be used to analyze metals or alloys because the incident beam mainly reflects without scattering. It can also be difficult to measure small concentrations of materials in a mixture because of the low rate of Stokes scattering.

Raman spectroscopy is useful for determining how many layers are present in a given sample of graphene because it provides recognizable frequency signatures for small multiples of graphene layers and other carbon allotropes like carbon nanotubes. This is done by comparing the heights and positions of the "so-called" D' and G spectral lines from each sample, which occur near the 2700 cm^{-1} and 1580 cm^{-1} positions in the spectra, [12, 13] (see Figure 5). Figure 6 shows the change in the D' line as the number of graphene layers in a sample is increased. The more layers there are, the more dominant the right peak in the chart; single-layer graphene has a single sharp D' peak, while the graphs for higher orders are clearly composed of two distinct peaks. Also, the more layers present in a sample, the further to the left the peak of the G line shifts. Beyond five or six graphene layers, samples produce spectrums that resemble that of the HOPG [2]; Raman is only capable of determining the number of layers present if there are fewer than five or six. All of these results agree with theory [3].

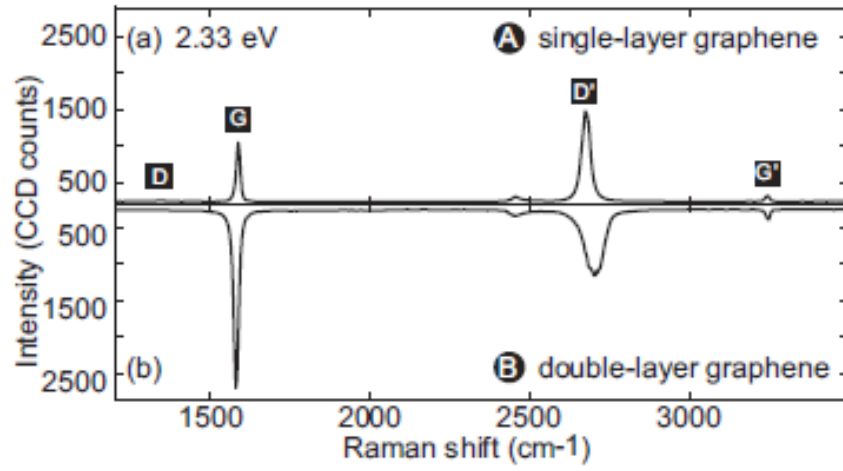


Figure 5: Raman spectra of A) single-layer and B) double-layer graphene [13]

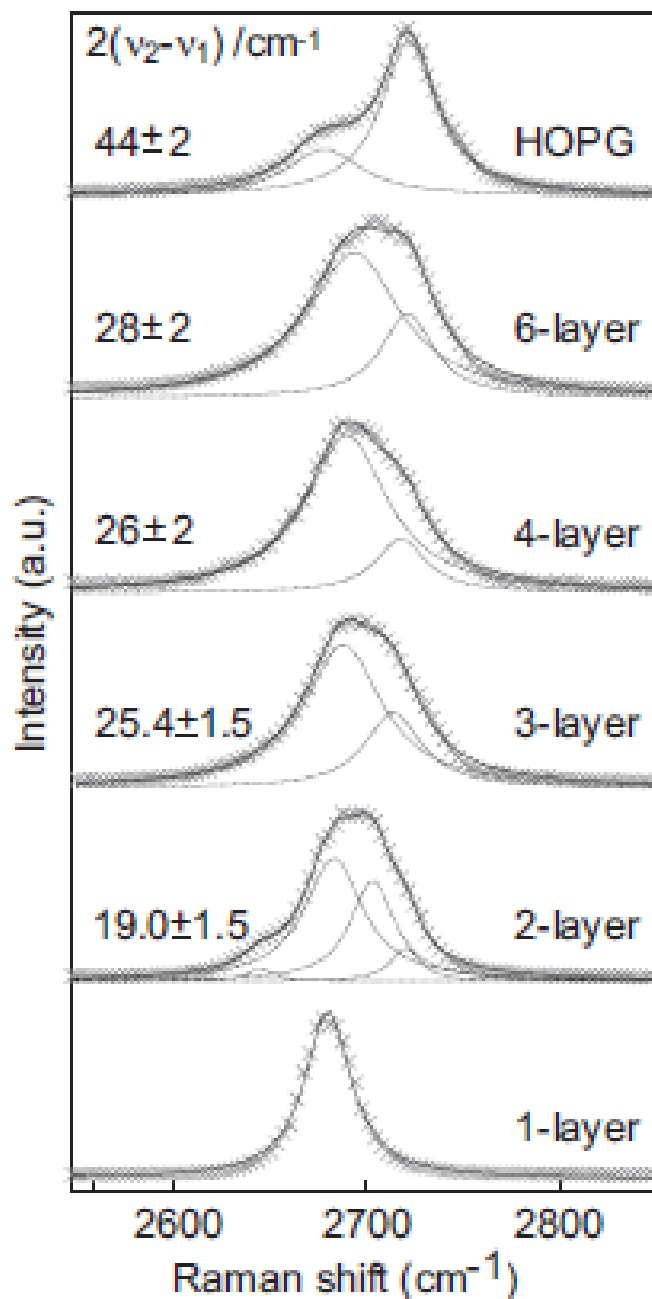


Figure 6: D' peak positions for varying numbers of graphene layers [13]

The setup for performing Raman spectroscopy is relatively straightforward (see Figure 7). Electromagnetic waves from a single-frequency source (such as a laser) are used to strike a sample of the material in question. The photons interact with molecules in the sample in the previously described manners, producing scattered photons of altered energies and wavelengths. These photons/waves are passed through a filter to reduce overlapping of the Raman signal with

that of Rayleigh scattering; interference notch filters are generally used. The waves then strike a diffraction grating, and the data read using charge-coupled devices (CCD's). Spectral resolution (the ability to separate and sharpen features within the spectrum) can be increased by increasing either the focal length or the grating used to disperse the spectrum.

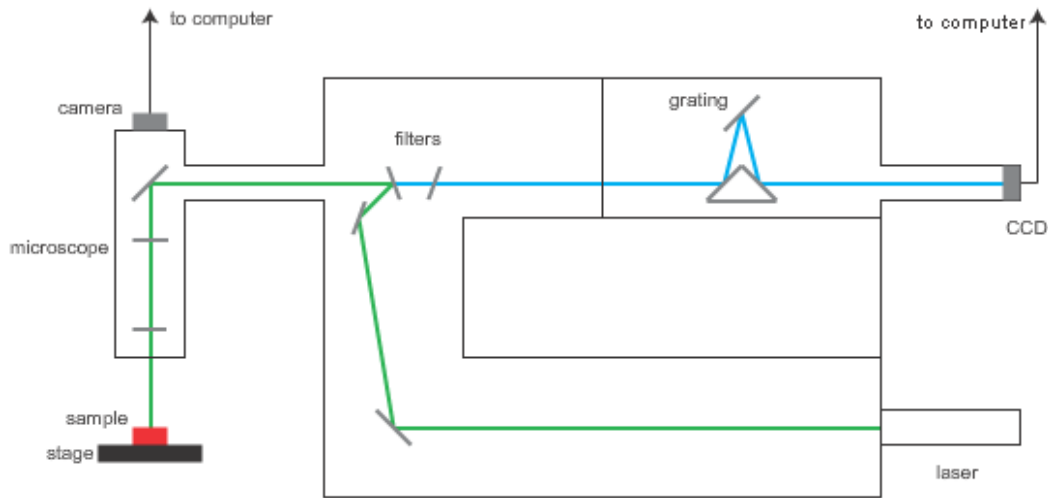


Figure 7: Setup for performing Raman spectroscopy

http://www.msm.cam.ac.uk/doitpoms/tplib/raman/raman_microspectroscopy.php

2. Experimental technique and procedure

a. Mechanical Exfoliation

This experiment utilized the method of mechanical exfoliation performed upon a wafer of HOPG (Figure 8), which is composed of many stacked layers of graphene. A diamond scribe was used to cut wafers of SiO_2 into small pieces roughly 5 mm^2 to be used as substrates for graphene. It has been determined in other work such as that of P. Blake et al. that 300 nm thick SiO_2 is ideal as a graphene substrate because it allows a single atom-layer of graphene to be visible with the naked eye under white light, unlike pure silicon's mirror-like surface [7]. The contrast between a graphene flake and a substrate has to be relatively high for the flake to be visible to the naked eye, which, in the case of a SiO_2 on Si substrate, relies on the relative indices of refraction of the SiO_2 , Si, and graphene. The behavior of light as it encounters each of these

transitions can be described using the Fresnel equations [7]. Indeed, the contrast was so high-quality that not only could graphene/graphite flakes be identified, but flakes with larger numbers of carbon layers appeared darker than those with fewer layers. According to Blake et. al, any thickness of SiO_2 will do when the right filters are used. About six inches of tape from a mount was discarded, including the piece of tape that had been exposed previously to the air collecting dust. A fresh piece was removed and pressed firmly adhesive-side down to the shiny side of the HOPG for about ten seconds. The tape was gently peeled away with thick, shiny layers of graphite stuck to it.



Figure 8: HOPG wafer

Next, the part of the tape with layers from the HOPG was refolded upon a clean adhesive section of the same piece of tape; the two layers were then pressed firmly together for several seconds. The tape was gently unfolded so that two mirrored graphite areas on the tape remained. This process was repeated with the original area removed from the HOPG on the tape until a large portion was no longer shiny, but dull, dark grey (see Figure 9). It was preferable that the area be more graphite and less bare tape so that more graphite and less glue residue would be transferred to the substrate; despite the fact that tape residue does not seriously affect the quality of the graphene flake samples, it does make those samples more difficult to find on the substrate. One of the small SiO_2 wafers was placed shiny-side down on that dull area with a pair of tweezers and pressed firmly to the tape for several seconds. It was then gently removed and placed in a labeled sample box. This process could be repeated separately for each SiO_2 wafer, or the same dull graphite area on the tape could be used for the production of several different wafers (maximum of two for this particular experiment).



Figure 9: Adhesive “Scotch” tape after being pressed to the HOPG and folded over several times upon itself.

Finally, each sample was individually placed underneath a Cambridge Instruments MicroZoom high-performance microscope at a magnification of 50x and methodically searched for graphite flakes thin enough to possibly be one layer thick. Likely “few-layers” flakes were identified by their particularly faint regions, indicating that few carbon layers were present. Once a likely flake was located, it was photographed using an MTI CCD72 camera attached to the microscope and saved using HrtDemo2001 software.

b. Raman Spectroscopy

By comparing the Raman spectra data for the samples in this experiment to the data found in previous experiments, the number of carbon sheet layers in each sample could be determined. This process was performed using Raman spectroscopy equipment made by Kaiser Optical Systems, Inc. at NASA Langley in Hampton, VA. First, the instrument was turned on so that the lasers could warm up. Next, the wavelength and spectrometer were calibrated using cyclohexane so that background wavelengths could be removed from the readout. Then a SiO₂ sample was placed in the machine under the microscope, focused, and searched until a desired graphite flake was found. The flake was photographed using the built-in color camera (see Figure 10 for an example), which had a higher resolution than the previous microscope camera used and could show fainter flake areas.

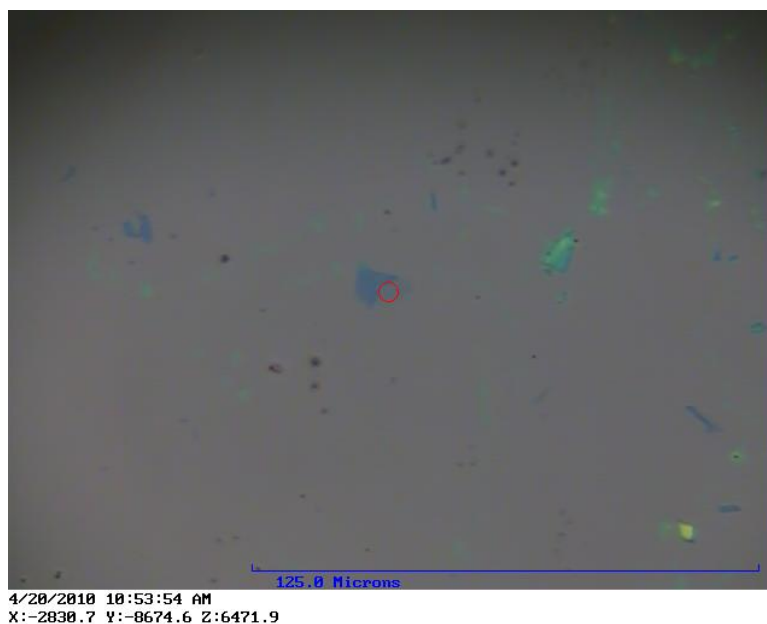


Figure 10: Graphite flake under color microscope

The area of the flake to be analyzed was centered upon (see Figure 10), the cover to the spectrometer closed, the white light turned off, and a barrier opened so that the laser beam used could strike the sample. A computer program then took fifty readings and combined them to produce a Raman shift chart.

Two such readings were taken of an HOPG and one reading each of five different flakes. Later, peaks in the spectrum shift data (the D' and G lines) from those readings were characterized using Lorentz distributions, which provided information on the structure of those regions. From this data hypotheses could be made concerning the number of graphene layers present in each flake sample.

3. Experimental data and data analysis

During the first semester, eight samples on SiO_2 were produced. Of the earlier samples, two did not produce any flakes likely to have graphene sections, which was probably due to a lack in experience in production. Of the six remaining samples, all produced flakes that could possibly include graphene sections, which resulted in 17 likely flakes with 9 of those having areas of a significant size. The largest region of possible single-layer graphene had a width of 17 μm . This was determined by taking an image using an optical microscope the tip of a cantilever

used for atomic force microscopy (AFM) and comparing its width in the image to the flake images. Please see Appendix A for a selection of photos of likely flake regions.

During the second semester, an HOPG and two SiO₂ sample chips were taken to NASA Langley and analyzed using Raman spectroscopy with two different laser wavelengths. The G and D' lines (roughly representing peaks located at 1580 cm⁻¹ and 2700 cm⁻¹) in the resulting spectrums were fitted with Lorentzian functions in order that the locations of the peaks of the function might be identified. The locations of these peaks, and the corresponding shapes of the D' lines, were compared to those in Figures 6 and 5. These showed that, in this experiment, the smallest number of graphene layers found in a flake was two. An example of a probable two-layer flake area is shown in Figures 11 and 12.

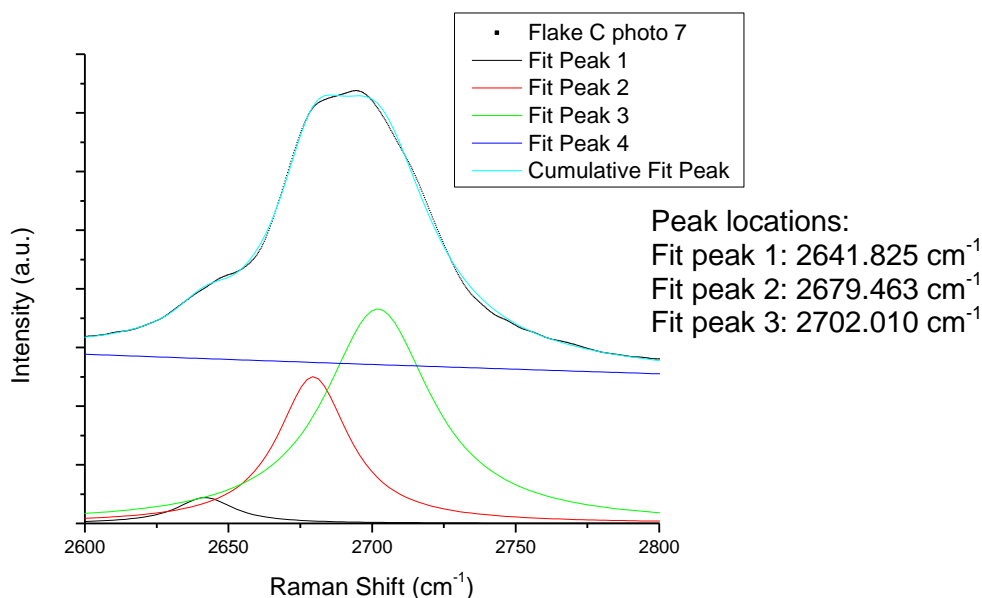


Figure 11: Fittings and peak locations for the D' line of two layers of graphene

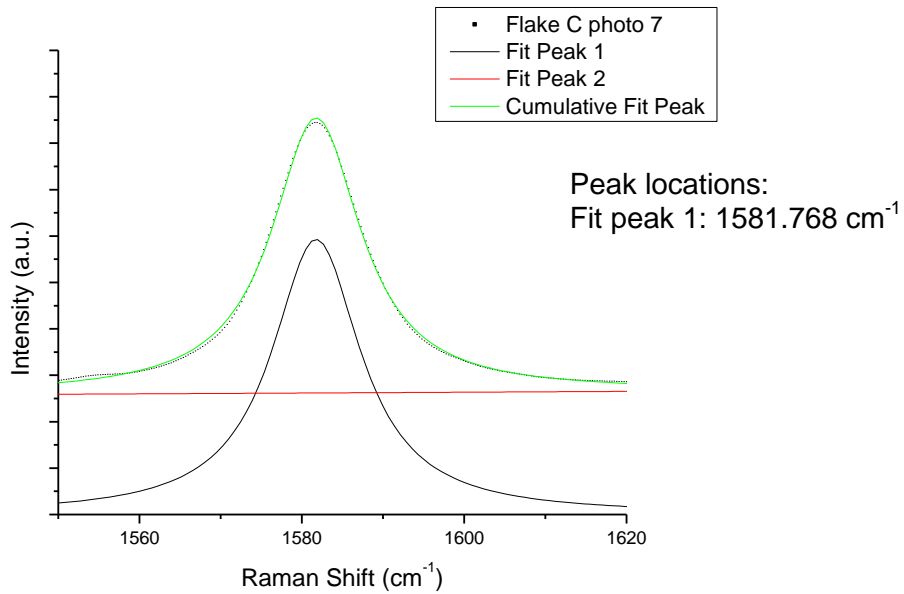


Figure 12: Fittings and peak location for the G line of two layers of graphene

The cumulative line in Figure 11 is very similar to the chart for two-layer graphene in Figure 6. Also, the location of the peak in Figure 12 is sufficiently greater than 1580 cm^{-1} to indicate a low number of layers. The difference is clear when compared to the charts and peak locations for the spectrum shift of the HOPG in Figures 13 and 14.

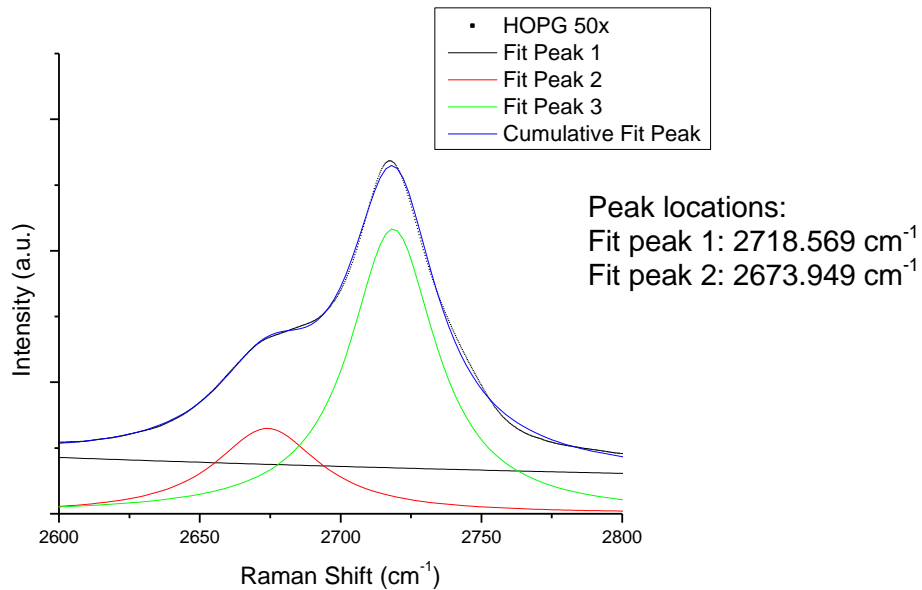


Figure 13: Fittings and peak locations for the D' line of the HOPG

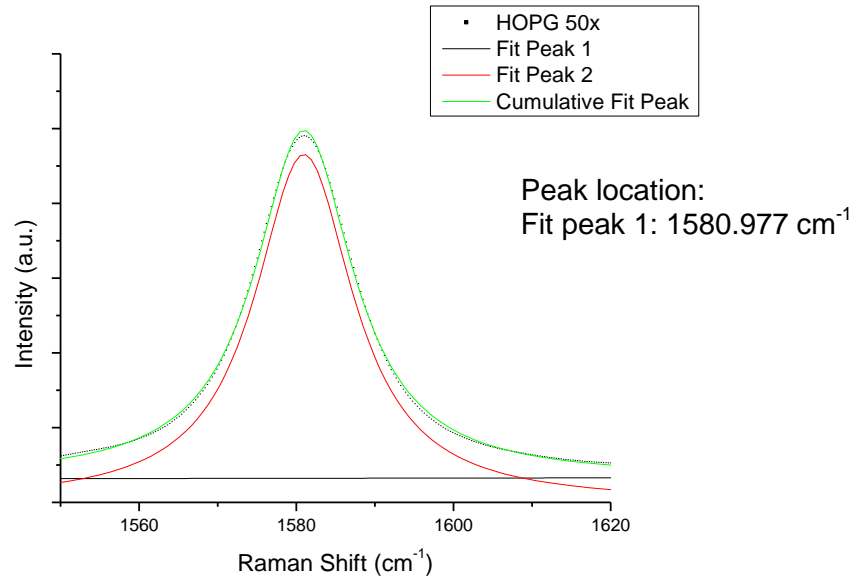


Figure 14: Fittings and peak location for the G line of the HOPG

A chart similar to that in Figure 6 showing the shift in shape of the D' line and giving a rough estimate of the number of graphene layers present can be made using the data gathered in this experiment (see Figure 15).

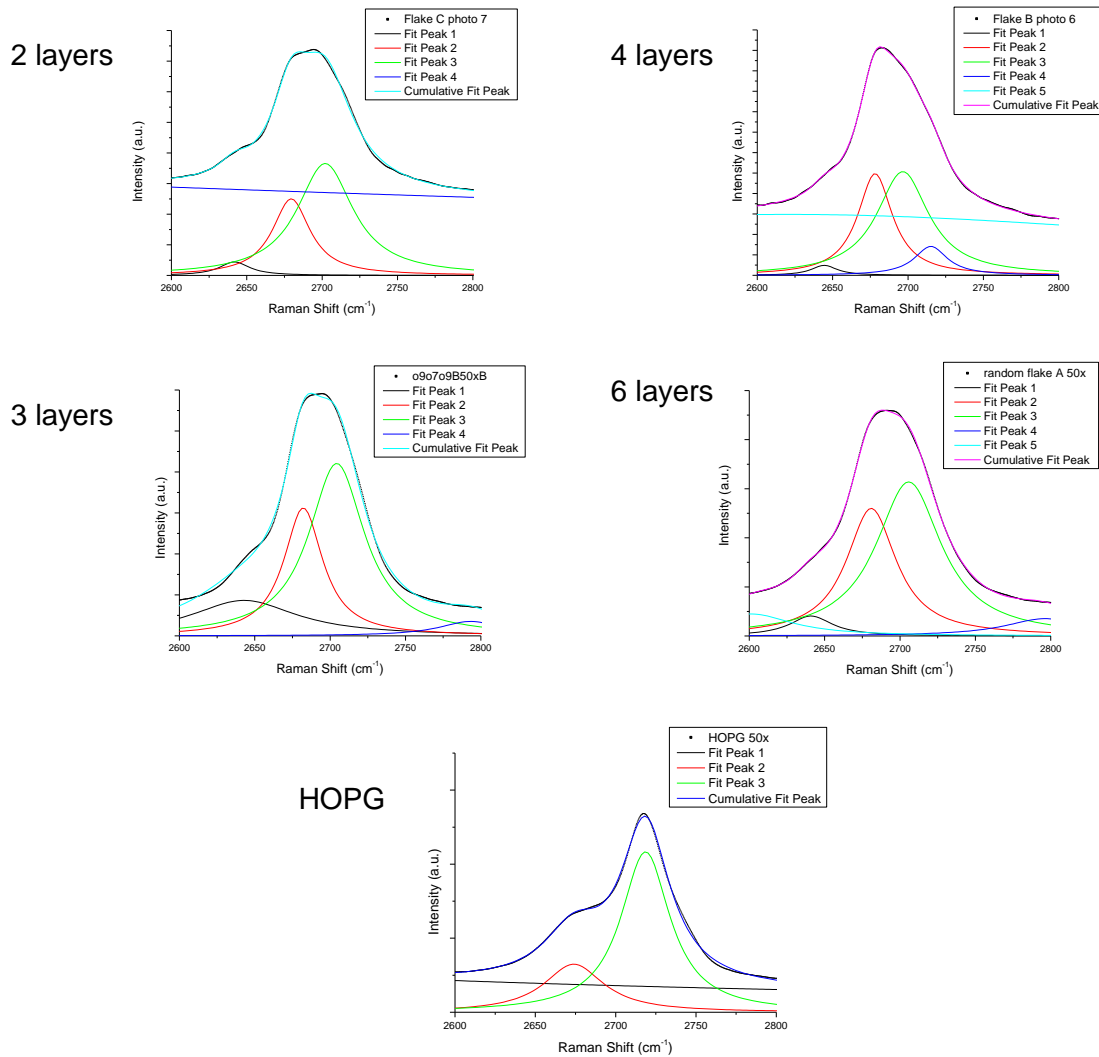


Figure 15: The transformation in the D' line as the number of graphene layers increase

4. Future research

In the future, it would be interesting to use the Raman method on graphene produced via methods besides mechanical exfoliation, including epitaxial growth on SiC, and compare the results with that found in this experiment in order to determine which method produces more areas of single-layer graphene. In addition, it will be useful to investigate differences in electron mobility in similar samples prepared with these two methods to elucidate possible mechanisms that hinder the predicted high mobility.

5. Acknowledgements

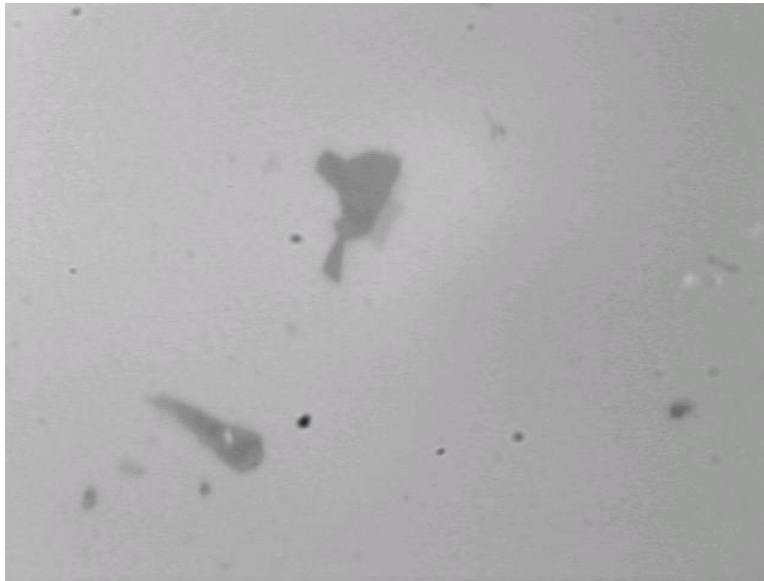
I would like to thank my research advisor, Professor Ale Lukaszew, and graduate student Will Roach for their help and guidance throughout this project. I would also like to thank Dr. Buzz Wincheski from NASA LaRC for his help in performing the Raman spectroscopy portion of this experiment.

6. References

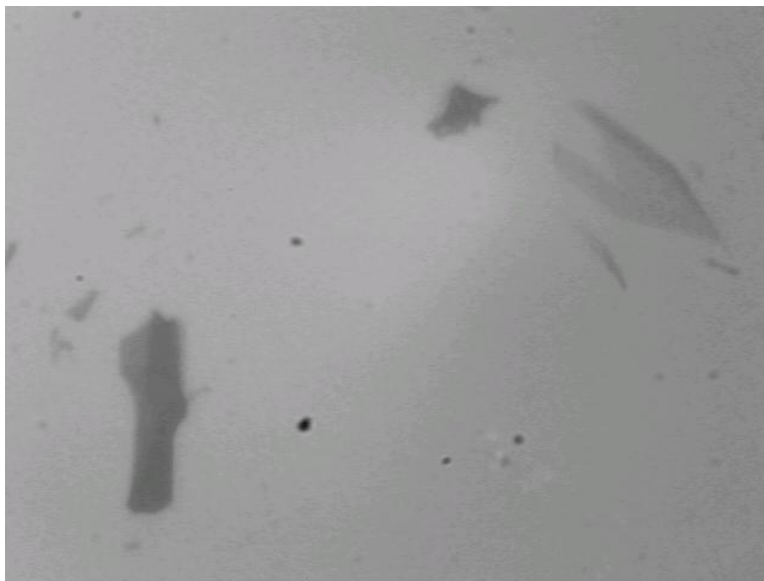
- [1] K. S. Novoselov *et al.* *Proc. Natl. Acad. Sci. U.S.A.* **102**, 10451 (2005).
- [2] Ferrari, A. *Solid State Communication* **143**, 47-57 (2007).
- [3] Reich, S. and Thomsen, C. *Philosophical Transactions: Mathematical, Physical and Engineering Sciences* **362**, 2271-2288 (2004).
- [4] Geim, A. K. and Novoselov, K. S. *Nature Materials* **169**, 183-191 (2007).
- [5] Kuzmenko, A. B.; van Heumen, E.; Carbone, F.; van der Marel, D. *Phys Rev Lett.* **100**, 117401 (2008).
- [6] Balandin, A.A. *et al.* *Nano Letters ASAP.* **8**, 902–7 (2008).
- [7] P. Blake, *et al.* *Appl. Phys. Lett.* **91**, 063124 (2007).
- [8] Kedzierski, J. *et. al.* *IEEE Transactions on Electron Devices* **55**, 2078-2085 (2008).
- [9] Stoller, M. D., Park, S., Zhu, Y., An, J., and Ruoff, R. S. *Nano Lett* **8**, 3498–3502 (2008).
- [10] Prawer, S. and Nemanich, R. J. *Philosophical Transactions: Mathematical, Physical and Engineering Sciences* **362**, 2537-2565 (2004).
- [11] Zhao, Q. and Wagner, H. D. *Philosophical Transactions: Mathematical, Physical and Engineering Sciences* **362**, 2407-2424 (2004).
- [12] Ferrari, A. C. *et al.* *Phys. Rev. Lett.*, **97**, 187401 (2006).
- [13] D. Graf, *et al.* *Nano Lett.* **7**, 238-42 (2007) .

Appendix A

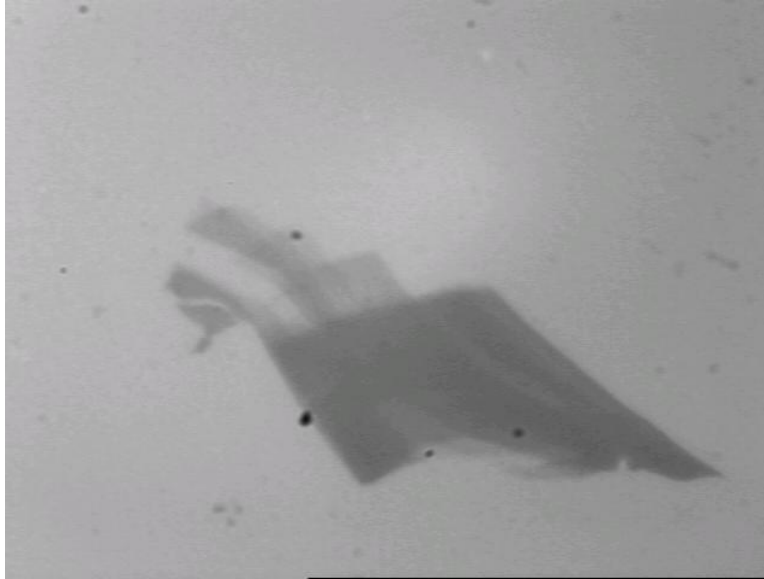
Graphite/graphene flakes produced in this experiment
All photos taken at a magnification of 50x using an optical microscope



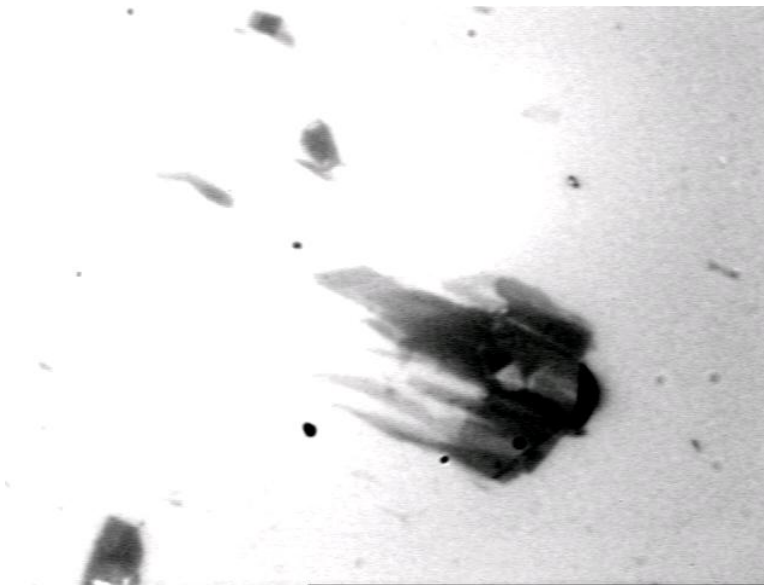
Sample 090709B, graphite flake 090709B50XA



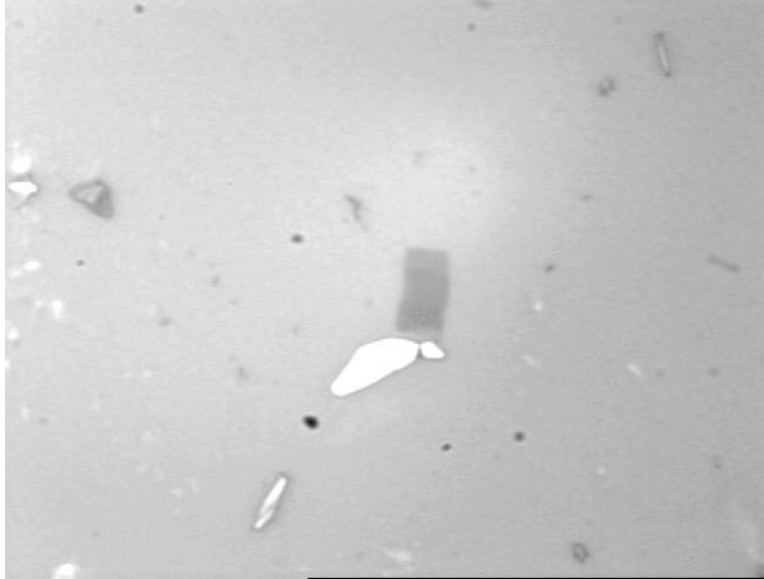
Sample 090709B, graphite flake 090709B50XB



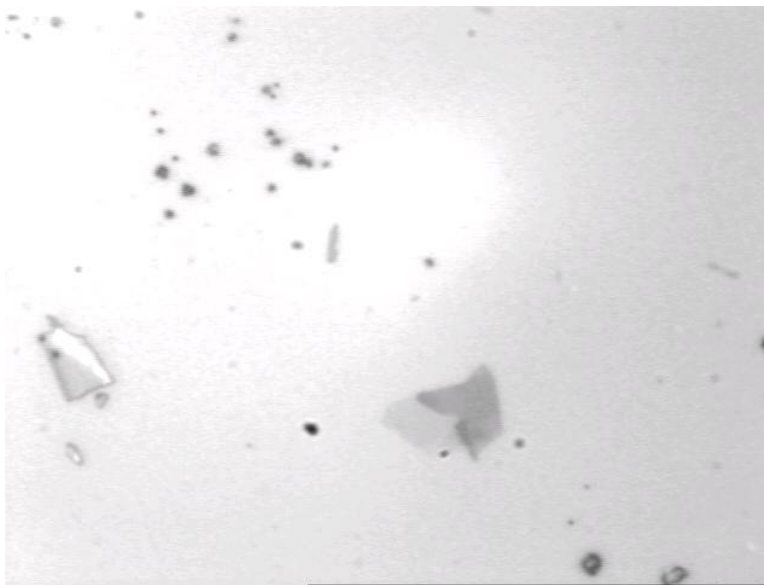
Sample o9o7o9B, graphite flake o9o7o9B50XD



Sample o914o9B, graphite flake o914o9B50XA



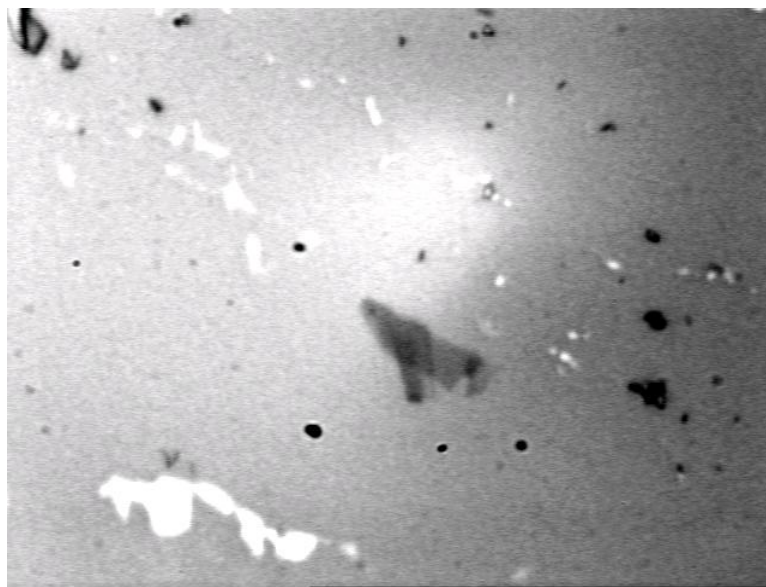
Sample o914o9B, graphite flake o914o9B50XD



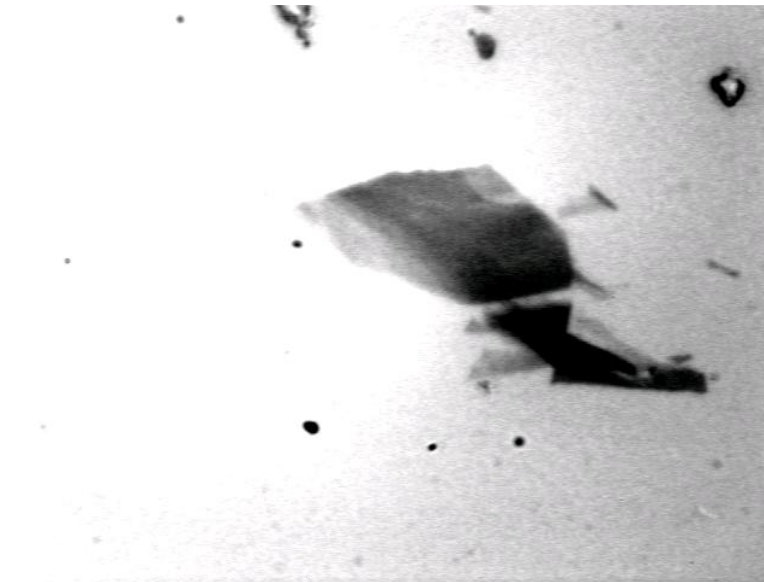
Sample o914o9B, graphite flake o914o9B50XE



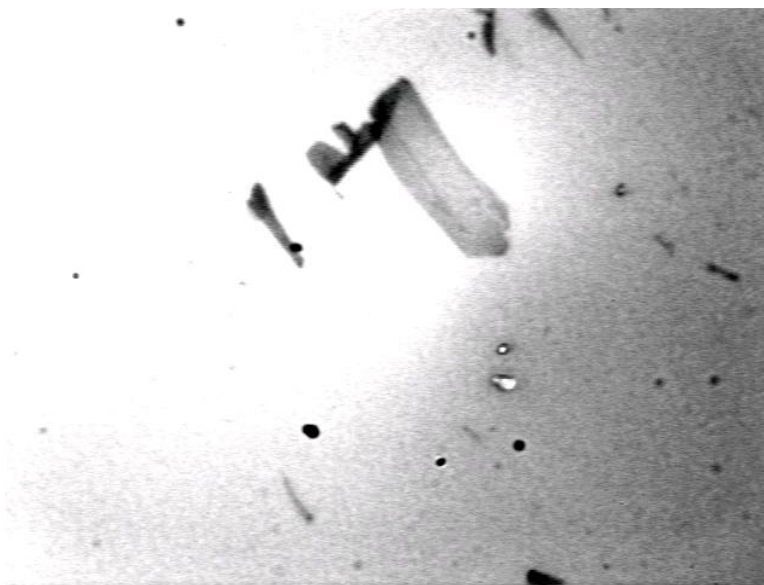
Sample o923o9B, graphite flake o923o9B50XA



Sample 1019o9A, graphite flake 1019o9A50XB



Sample 1019o9A, graphite flake 1019o950XC



Sample 1019o9A, graphite flake 1019o9A50XD



Sample 1019o9A, graphite flake 1019o950XE